

Single π^0 production in μe scattering at MUonE

Ettore Budassi^{a,b}, Carlo M. Carloni Calame^b, Clara Lavinia Del Pio^{a,b}, Fulvio Piccinini^b

^a*Dipartimento di Fisica, Università di Pavia, Via A. Bassi 6, 27100, Pavia, Italy*

^b*INFN, Sezione di Pavia, Via A. Bassi 6, 27100, Pavia, Italy*

Abstract

The recently proposed MUonE experiment at CERN aims at providing a novel determination of the leading order hadronic contribution to the muon anomalous magnetic moment through the study of elastic muon-electron scattering at relatively small momentum transfer. The anticipated accuracy of the order of 10ppm demands for high-precision prediction in radiative corrections to the μe scattering as well as for robust quantitative estimates of all possible background processes. In this letter, the contribution due to the emission of a neutral pion through the process $\mu e \rightarrow \mu e \pi^0$ is studied and its numerical impact is discussed in different phase space configurations by means of the upgraded Monte Carlo event generator MESMER. In fact, single π^0 production could be a source of reducible background for the measurement of the QED running coupling constant at MUonE and it could be also an important background for possible New Physics searches at MUonE involving $2 \rightarrow 3$ processes, in phase space regions complementary to the ones characteristic of the elastic μe scattering.

Keywords: Fixed target experiments, Monte Carlo simulations, QED

1. Introduction

The value of the anomalous magnetic moment of the muon, $a_\mu = (g - 2)_\mu/2$, is a fundamental quantity in particle physics. Very recently, the measurement performed by the Fermilab Muon $g - 2$ Experiment (E969) [1] has been combined with the Brookhaven National Laboratory result of 2001 [2], yielding a deviation of 4.2σ from the theoretical prediction of the muon anomaly, which stems from the QED, weak and strong sectors of the Standard Model (SM) [3, 4]. The current status of the SM theoretical prediction for the muon $g - 2$ has been recently reviewed in Ref. [5]. The comparison between theory and experiment provides a stringent test of the SM: indeed, a deviation from the SM expectation can point to possible New Physics signals.

The dominant contributions to the theoretical error comes from Leading Order Hadronic Vacuum Polarisation (HLO) and Hadronic Light by Light (HLbL) effects, the latter having less impact [5]. Concerning the HLO term, the BMW collaboration has recently presented a precise determination of a_μ^{HLO} , based on Lattice QCD calculations, with an uncertainty of 0.78% [6] and a central value larger than the ones obtained via dispersive techniques, which typically allow to achieve the highest available precision in a_μ^{HLO} . The discrepancy between the BMW a_μ^{HLO} estimate, which would lead to an a_μ prediction in agreement with the BNL and FNAL experimental determinations [1, 2], and the a_μ^{HLO} results based on dispersion relations ranges from 2 to 2.5σ , depending on the reference value used for the dispersive approach. In order to clarify this tension and in view of the importance of a very robust theoretical SM prediction for a_μ , alternative and independent methods for the evaluation of a_μ^{HLO} are therefore more than welcome, if not necessary.

Recently, a novel approach has been proposed in Ref. [7] to derive a_μ^{HLO} from a measurement of the effective electromagnetic coupling constant in the space-like region via scattering data, making use of

Email addresses:

ettore.budassi01@universitadipavia.it (Ettore Budassi), carlo.carloni.calame@pv.infn.it (Carlo M. Carloni Calame), claralavinia.delpio01@universitadipavia.it (Clara Lavinia Del Pio), fulvio.piccinini@pv.infn.it (Fulvio Piccinini)

a relation between $\Delta\alpha_{\text{had}}(q^2)$ at negative squared momenta and a_μ^{HLO} (see also [8])¹. Shortly afterwards, the elastic scattering of muons on electrons has been identified as an ideal process for such a measurement [10]² and a new experiment, MUonE, has been proposed at CERN to measure the differential cross section of this process [14]. In order for this new determination of a_μ^{HLO} to be competitive with the traditional dispersive approach, the uncertainty in the measurement of the μe differential cross section must be of the order of 10ppm, as described in Refs. [10, 14].

Such a target precision is extremely challenging on both the experimental as well as the theoretical side. Recent progress, after the experimental proposal [14], in the study of the main systematics and in the development of the experimental apparatus and data analysis strategies have been documented in Refs. [15, 16, 17, 18, 19, 20]. On the theory side several groups have already reached important milestones related to next-to-next-to-leading QED radiative corrections and their implementation in independent MC codes [21, 22, 23, 24, 25, 26, 27, 28, 29].

In this paper we focus on hadronic corrections, whose virtual part has already been studied in Refs. [30, 31]. The real-emission contributions consist of three channels: $\mu^\pm e \rightarrow \mu^\pm e \pi^+ \pi^-$, $\mu^\pm e \rightarrow \mu^\pm e \pi^0 \pi^0$ and $\mu^\pm e \rightarrow \mu^\pm e \pi^0$ ³. While pion-pair production is extremely constrained for the limited available phase space at MUonE, since, as already noted in Ref. [28], a realistic event selection makes the cross section vanishing, the single pion production channel deserves a more detailed investigation. In fact, while on dimensional grounds the impact of pion emission in μe scattering is expected to be suppressed w.r.t. the elastic scattering, the π^0 production is dynamically enhanced in the region of small electron and muon scattering angles. In this region, which is particularly interesting for MUonE, the elastic cross section becomes negligi-

ble and the sensitivity to the running of the electromagnetic coupling constant reaches its maximum. Since the MUonE experimental apparatus relies primarily on high-resolution charged track reconstruction, the two photons which the π^0 decays into are not detected. Hence, the signature of the process under study corresponds to the one of the elastic $\mu^\pm e \rightarrow \mu^\pm e$ process: this fact reflects the importance of studying the π^0 production process.

An additional reason for a detailed study of the process $\mu^\pm e \rightarrow \mu^\pm e \pi^0$ at MUonE is its potential role as a background to possible New Physics searches in phase space regions that are complementary to the ones which characterise the elastic scattering. On the one hand, according to the findings of Refs. [32, 33], μe elastic scattering at MUonE is insensitive to possible New Physics contamination. On the other hand, at MUonE it could be possible to have sensitivity to the production of a light new gauge boson Z' through the process $\mu^\pm e \rightarrow \mu^\pm e Z'$ [34] or to the production of a dark photon through the process $\mu^\pm e \rightarrow \mu^\pm e A'$ [35]. It has to be noted that for this kind of searches additional future studies on the experimental apparatus may be probably needed.

In Section 2 we give a brief description of the tree-level matrix element and phase space (PS) calculation, which are implemented as an additional channel in the Monte Carlo generator MESMER [22, 26, 28]⁴ and in Section 3 we present some numerical results for the two above mentioned complementary event selections: in Section 3.1 the differential distributions relevant for the background to the μe elastic scattering are examined, while Section 3.2 presents few results relevant for the event selection envisaged in Ref. [34] for the search of a light $L_\mu - L_\tau$ gauge boson. Section 4 summarises our study.

2. Calculation

The process under study is:

$$\mu^\pm(p_1)e(p_2) \rightarrow \mu^\pm(p_3)e(p_4) + \pi^0(p_5), \quad (1)$$

where p_i are the four-momenta of the particles.

In order to determine the numerical impact of the $\mu^\pm e \rightarrow \mu^\pm e \pi^0$ process, the tree-level scattering amplitude and the three-body PS have been calculated

¹Very recently, analytic expressions have been provided in Ref. [9] to extend the space-like calculation of the hadronic vacuum polarization contribution to a_μ up to next-to-leading order precision.

²A method to measure the running of the QED coupling constant in the space-like region using small-angle Bhabha scattering was proposed in Ref. [11] and applied to LEP data by the OPAL Collaboration [12]. In the time-like region, the effective QED coupling constant in the region below 1 GeV has been recently measured by the KLOE Collaboration [13].

³The need for a quantitative estimate of these contributions was firstly stressed in Ref. [25].

⁴An up-to-date version of MESMER can be found at www.github.com/cm-cc/mesmer.

and implemented in the Monte Carlo event generator MESMER. To derive the former, we started from the $\pi^0\gamma\gamma$ interaction Lagrangian density:

$$\mathcal{L}_1 = \frac{g}{2!} \varepsilon^{\mu\nu\kappa\lambda} F_{\mu\nu} F_{\kappa\lambda} \varphi_\pi, \quad (2)$$

where a form factor $F_{\pi^0\gamma^*\gamma^*}(p^2, q^2)$ dependent on the photon virtualities, p^2 and q^2 , is understood, as in Ref. [36]. We then computed the vertex Feynman rule, $-4ig\varepsilon_{\mu\rho\nu\sigma}p^\rho q^\sigma F_{\pi^0\gamma^*\gamma^*}(p^2, q^2)$, where p^ρ and q^σ are the four-momenta of the photons. To obtain the $\pi^0\gamma^*\gamma^*$ coupling value, we exploited the relation between g and the π^0 decay width

$$g^2 = \frac{4\pi\Gamma_{\pi^0\rightarrow\gamma\gamma}}{m_{\pi^0}^3}, \quad (3)$$

as in Ref. [36]. In Eq. (3) m_{π^0} is the mass of the neutral pion, 134.9766 MeV [37], and the decay width is related to the f_π parameter by:

$$\Gamma_{\pi^0\rightarrow\gamma\gamma} = \frac{\alpha^2 m_{\pi^0}^3}{64\pi^3 f_\pi^2}.$$

By using for f_π the value adopted in fit 1 in Table II of Ref. [38], $f_\pi = 0.092388$ GeV, the corresponding π^0 width is $\Gamma_{\pi^0\rightarrow\gamma\gamma} = 7.731$ eV, to be compared with the experimentally measured value $\Gamma_{\pi^0\rightarrow\gamma\gamma} = 7.802 \pm 0.052 \pm 0.105$ eV [39]. The exact tree-level matrix element for the process $\mu e \rightarrow \mu e \pi^0$ (Fig. 1 shows the corresponding Feynman diagram) has been obtained by means of the symbolic manipulation program FORM [40, 41, 42], keeping all finite mass contributions.

From now on we do not specify the electric charge of the incoming muons because the cross section with unpolarized muons is the same for μ^+ and μ^- .

The form factor $F_{\pi^0\gamma^*\gamma^*}$ has been calculated according to the resonance chiral symmetric model with $SU(3)$ breaking of Ref. [38]. In particular, we implemented the expression of Eq. (14) of Ref. [38] with three octets and the values of the parameters taken from Table II, column fit 1, of the same reference.

Concerning the PS parameterisation, we decomposed the three-body Lorentz-invariant phase space

$$d\Phi_3^{\text{LIPS}} = \int \prod_{i=3}^5 \frac{d^3 p_i}{(2\pi)^3 2E_i} \delta^4 \left(P - \sum_{j=3}^5 p_j \right). \quad (4)$$

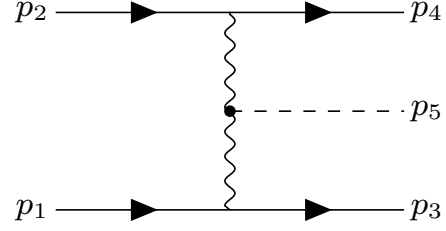


Figure 1: The tree-level Feynman diagram for the process $\mu e \rightarrow \mu e \pi^0$. The particle labels follow the convention of Eq. 1.

according to the following chain:

$$d\Phi_3^{\text{LIPS}} = (2\pi)^3 \int dQ^2 d\Phi_2(P \rightarrow p_3 + Q) \times d\Phi_2(Q \rightarrow p_4 + p_5), \quad (5)$$

where the particle labels 3, 4 and 5 stand for final state μ , e and π^0 , respectively. The set of independent variables generated for this parameterisation is given by:

$$\vartheta_\mu, \varphi_\mu, Q^2, \vartheta_e^*, \varphi_e^*,$$

where ϑ_e^* and φ_e^* are generated in the rest frame of the pair 45 ($\vec{p}_4 + \vec{p}_5 = \vec{0}$). The sampling of the variables ϑ_μ and ϑ_e^* follows the same approach of Ref. [28], inspired by Refs. [43, 44].

As a cross check of our Monte Carlo results, we reproduced the results of Table 1 of Ref. [36] on the total cross section of the process $e^+e^- \rightarrow e^+e^-\pi^0$, by setting $m_\mu = m_e$ and adjusting the incoming e^+ beam energy to reproduce the centre of mass energies of Table 1 of Ref. [36]. It is worth mentioning that the state of the art for the Monte Carlo simulation of the process $e^+e^- \rightarrow e^+e^-\pi^0$ is represented by the event generator EKHARA [45, 46]. By means of a tuned comparison, we obtained excellent agreement between our prediction for the “ t -channel” cross section of the process $e^+e^- \rightarrow e^+e^-\pi^0$ and the results for the same cross section obtained with EKHARA.

The above described calculation has been implemented in MESMER and in an independent Monte Carlo program for the cross-check of the numerical results, which we present in the following section.

3. Numerical Results

In this section we investigate the numerical impact of π^0 production in μe scattering for typi-

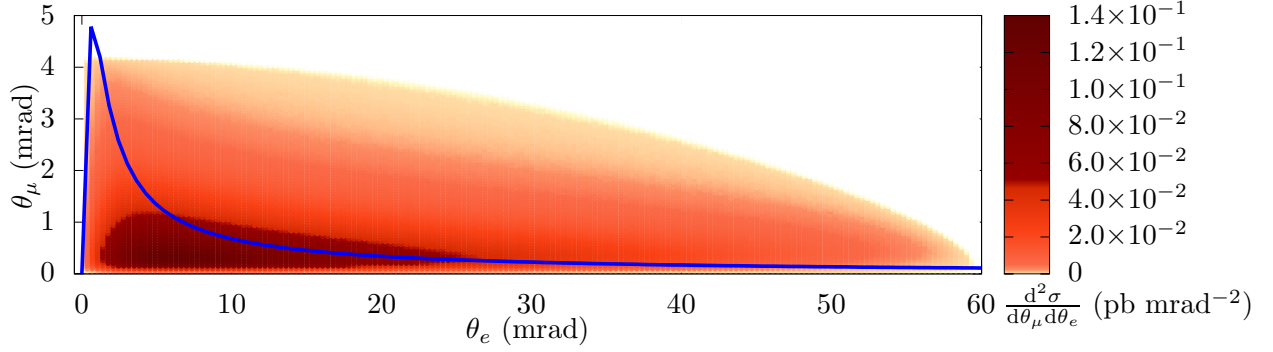


Figure 2: The configuration space for the $\mu e \rightarrow \mu e \pi^0$ process in terms of the outgoing particle angles ϑ_e (on the x axis) and ϑ_μ (on the y axis) with *basic acceptance cuts*. The colour gradient represents the doubly differential cross section $d^2\sigma/d\vartheta_e d\vartheta_\mu$ (in pb mrad^{-2}): the darker the colour, the higher the cross section. In blue, we show the elasticity curve as defined in Eq. (5.1) of Ref. [28].

cal running conditions and event selections of the MUonE experiment. In particular, we consider in Section 3.1 the process $\mu e \rightarrow \mu e \pi^0$ as a possible reducible background to the determination of the running of the electromagnetic coupling constant in the space-like channel through the measurement of the differential cross section of the elastic process $\mu e \rightarrow \mu e$. In Section 3.2 we discuss the impact of π^0 production as a possible background to New Physics searches in $2 \rightarrow 3$ channels.

3.1. Background to μe scattering

The numerical impact of π^0 production in μe scattering at MUonE is expected to be suppressed with respect to the μe elastic scattering: indeed, by dimensional analysis, the pion production cross section is reduced w.r.t. the tree level one at least by a factor of the order of $g^2 m_\pi^2 \sim 10^{-6}$, where m_π is the π^0 mass and g is the $\pi^0 \gamma^* \gamma^*$ coupling.

Using the same numerical values for the parameters α , m_e and m_μ as in Refs. [22, 26, 28] and $m_\pi = 134.9766$ MeV [37], the total cross section for the process $\mu e \rightarrow \mu e \pi^0$ with incoming muon energy of 150 GeV and initial-state electron at rest is:

$$\sigma_{\mu e \pi^0} = 6.53589(6) \text{ pb.}$$

With the two different event selections considered in previous studies on radiative corrections to the elastic process [22, 26, 28], namely

- *basic acceptance cuts*: $\vartheta_\mu \lesssim 4.84$ mrad, $E_\mu \gtrsim 10.28$ GeV, $\vartheta_e < 100$ mrad and $E_e > 0.2$ GeV,
- the same basic acceptance cuts, but with $E_e > 1$ GeV,

we obtain

$$\sigma_{\mu e \pi^0}^{0.2 \text{ GeV}} = 2.69836(4) \text{ pb,}$$

and

$$\sigma_{\mu e \pi^0}^{1 \text{ GeV}} = 1.61597(3) \text{ pb,}$$

respectively. With a tree-level elastic cross section $\sigma \sim 1265 \mu\text{b}$ for $E_e > 0.2$ GeV and $\sigma \sim 245 \mu\text{b}$ for $E_e > 1$ GeV, it is unlikely that π^0 production is numerically relevant for the determination of the running QED coupling constant at MUonE. However, in order to completely exclude possible enhancements of π^0 production in some phase space regions⁵, we present also numerical results at the differential level. In Fig. 2 we present the doubly differential distribution $d^2\sigma/d\vartheta_e d\vartheta_\mu$, where, by inspection, the leading contribution to the cross section is concentrated in the region $\vartheta_\mu \lesssim 1$ mrad and $\vartheta_e \lesssim 25$ mrad, which overlaps with the correlation curve $\vartheta_\mu(\vartheta_e)$ of the μe elastic scattering process (blue line) for electron scattering angles larger than about 5 mrad.

In order to clearly illustrate the contribution of π^0 production w.r.t. the elastic μe scattering for some key differential distributions, i.e. electron and muon scattering angles in the laboratory frame and squared transferred momentum along the electron line (t_{ee}) and along the muon line ($t_{\mu\mu}$), we consider the differential ratio of the π^0 production cross section with the tree-level prediction for $\mu e \rightarrow \mu e$:

$$K_{\pi^0} = \frac{d\sigma_{\mu e \pi^0}}{d\sigma_{\mu e}}. \quad (6)$$

⁵For instance, in the region $\vartheta_e \rightarrow 0$, where the elastic cross section becomes vanishingly small [22].

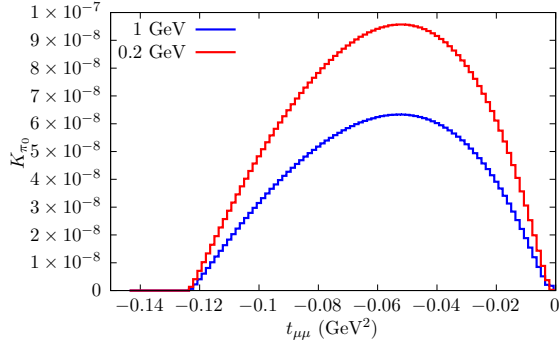


Figure 3: The K factor, K_{π^0} , as defined in Eq. (6) plotted against the transferred momentum along the muon line $t_{\mu\mu}$.

In all the remaining figures presented in this section, the blue histograms display K_{π^0} calculated with the threshold on the electron energy of 1 GeV while the red histograms refer to the electron energy threshold of 0.2 GeV.

Fig. 3 shows K_{π^0} plotted against $t_{\mu\mu}$, where the π^0 production weighs at most about 10^{-7} and 6×10^{-8} with $E_e > 0.2$ GeV and $E_e > 1$ GeV, respectively. The effect remains well below 10 ppm also in the K factor plotted against t_{ee} , as displayed in Fig. 4. K_{π^0} remains below 2.5×10^{-8} in the whole range of t_{ee} .

In Figs. 5 and 6, the K factors K_{π^0} are shown in terms of the outgoing electron and muon angles, respectively. The scattering angles are defined in the laboratory reference frame. Also in these plots the effects of π^0 production stay below 2.6×10^{-7} and 1.3×10^{-7} respectively, and thus are clearly negligible with respect to the 10 ppm level target precision of MUonE.

From this analysis, we can safely conclude that the process $\mu e \rightarrow \mu e \pi^0$ does not represent a signifi-

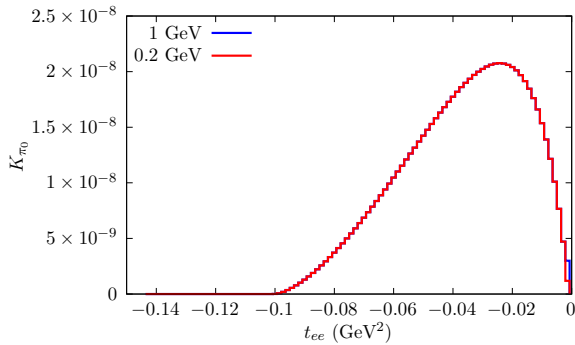


Figure 4: The same as in Fig. 3 but plotted against the squared momentum transfer along the electron line t_{ee} .

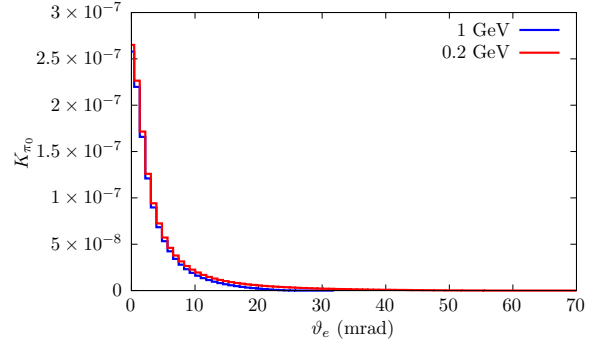


Figure 5: The same as in Fig. 3 but plotted against the outgoing electron angle in the laboratory reference frame ϑ_e .

cant source of background for the extraction of the hadronic contribution to the running of the electromagnetic coupling constant at the MUonE experiment at the target level of precision.

3.2. Background to New Physics search with $2 \rightarrow 3$ processes

As discussed in the Introduction, the process $\mu e \rightarrow \mu e \pi^0$ could represent a source of background for possible New Physics searches at MUonE in $2 \rightarrow 3$ processes, recently discussed, for instance, in Refs. [34, 35]. We consider in some detail the example suggested in Ref. [34], within the context of a $L_\mu - L_\tau$ gauge model, where a light massive Z' could be directly produced through the process $\mu e \rightarrow \mu e Z'$, with subsequent decay of Z' to a neutrino pair. In this case, π^0 production would be a reducible background, since the pion decays into two photons with Branching Ratio (BR) $\sim 98.8\%$ [39]⁶. We will assume in our simulation $BR(\pi^0 \rightarrow \gamma\gamma) = 1$.

For the sake of illustration, we study the numerical impact of π^0 production at MUonE with the event selection suggested in Ref. [34]:

- $\vartheta_\mu > 1.5$ mrad;
- $E_e \in [1, 25]$ GeV .

This cut choice covers a PS region that is complementary to the one of interest for the $\mu e \rightarrow \mu e$ elastic process, discussed in the previous subsection, and could be relevant for the search of a light Z' , as discussed in Ref. [34]. The integrated cross section

⁶The π^0 production can be a source of reducible background to dark photon searches, as proposed in Ref. [35], through the decay channel $\pi^0 \rightarrow e^+ e^- \gamma$.

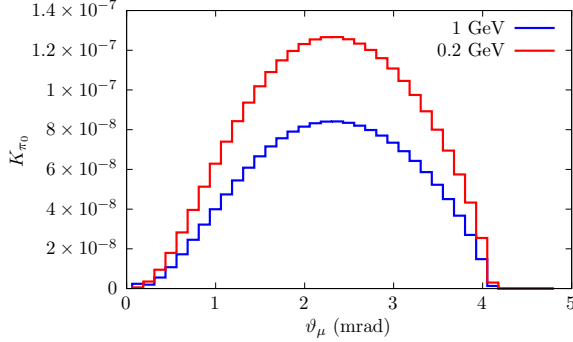


Figure 6: The same as in Fig. 3 but plotted against the outgoing muon angle in the laboratory reference frame ϑ_μ .

for π^0 production with the above event selection is:

$$\sigma_{\mu e \pi^0} = 0.19210(1) \text{ pb.} \quad (7)$$

Considering an integrated luminosity for the MUonE experiment of about 15 fb^{-1} as reported in Ref. [15], the number of expected events for the process $\mu e \rightarrow \mu e \pi^0$ is about 3×10^3 , which is of the same order of magnitude of the number of signal Z' events reported in Ref. [34]. Of course the impact of π^0 production can be reduced through a photon veto strategy. As already noted in Ref. [34], the main reducible background is expected to come from the radiative process $\mu e \rightarrow \mu e \gamma(\gamma)$. This could be studied in detail with the MC generator MESMER. In general, an efficient performance on photon identification and rejection would likely require some detector development with respect to its original proposal [14]. In the following, for the sake of

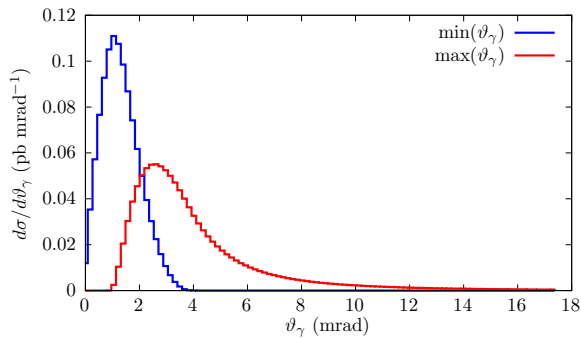


Figure 7: In blue, the differential cross section for the $\mu e \rightarrow \mu e + \pi^0 \rightarrow \mu e + \gamma\gamma$ process versus the minimum photon angle in the laboratory frame $\min(\vartheta_\gamma)$ is plotted. The red curve represents the same quantity but w.r.t. the maximum photon angle $\max(\vartheta_\gamma)$.

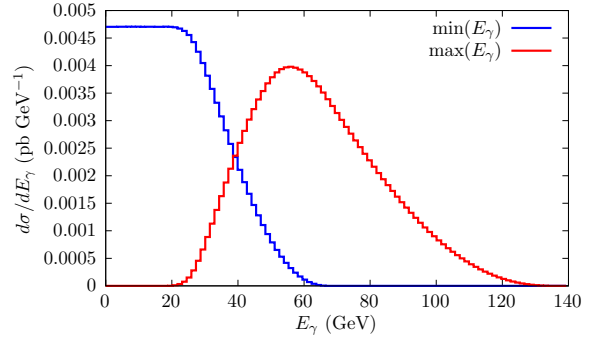


Figure 8: The same as in Fig. 7 but plotted against the minimum (blue curve) and the maximum (red curve) of the photon energy E_γ .

illustration, we present the features of the differential distributions of the photons originated from the π^0 decay, as obtained with the MC generator MESMER. In particular, we examine the differential distributions on angle and energy of the final state photons, on the invariant mass of the lepton-photon system as well as on the outgoing electron energy:

$$\frac{d\sigma}{dm_{e\gamma}}, \quad \frac{d\sigma}{dm_{\mu\gamma}}, \quad \frac{d\sigma}{dE_\gamma}, \quad \frac{d\sigma}{d\vartheta_\gamma}, \quad \frac{d\sigma}{dE_e}. \quad (8)$$

In Fig. 7 we show the differential cross section plotted against the photon angle ϑ_γ : it is clear that the photons are all produced in the forward region, below ~ 10 mrad in the laboratory reference frame. The minimum angle distribution has a very pronounced peak at about 1 mrad where the distribution reaches approximately $0.11 \text{ pb mrad}^{-1}$. Fig. 8 shows the minimum and maximum photon energy E_γ in the laboratory frame: the former remains constant at about $4.5 \times 10^{-3} \text{ pb GeV}^{-1}$ and then goes to zero approximately at 65 GeV. The maximum photon energy has about the same order of magnitude between 20 GeV and 130 GeV with a peak at 60 GeV.

We then turn our attention to the invariant mass of the lepton-photon system $m_{e\gamma}$. In Fig. 9 we plot the differential cross section over the minimum and maximum $m_{e\gamma}$ value: for each photon, it is calculated the invariant mass of the $e - \gamma$ system and then the minimum (maximum) is taken. The plot for the minimum value shows that $m_{e\gamma}$ stays between 0 GeV and 0.17 GeV with a peak that reaches about 2 pb GeV^{-1} . The distribution for the maximum of the $e - \gamma$ invariant mass is more spread out,

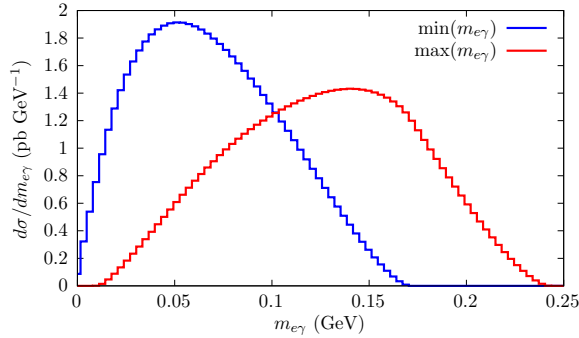


Figure 9: The same as in Fig. 7 but plotted against the minimum (blue curve) and the maximum (red curve) of the invariant mass of the $e - \gamma$ system $m_{e\gamma}$.

ranging from about 0 GeV to 0.25 GeV with a peak at 0.15 GeV of 1.4 pb GeV⁻¹.

The same line of reasoning is followed for the $\mu - \gamma$ system, with the results shown in Fig. 10. The distribution for the minimum of the invariant mass $m_{\mu\gamma}$ ranges between 0.1 GeV and 0.28 GeV, peaking at about 0.19 GeV with a value for the differential cross section of 1.8 pb GeV⁻¹. The $\max(m_{\mu\gamma})$ distribution ranges between 0.17 GeV and 0.38 GeV with a peak at about 0.27 GeV, where the distribution reaches 2 pb GeV⁻¹. Fig. 11 shows the distribution for the outgoing electron energy E_e . Given the event selection, the range of this observable is between 1 GeV and 25 GeV. The bulk of the events have small E_e : the peak of the differential cross section is approximately at 1.2 GeV, where it reaches almost 6×10^{-2} pb GeV⁻¹. This distribution has a shape qualitatively similar to the one of the signal process (cfr. Fig. 2 of Ref. [34]), with a more pronounced tail after the peak.

4. Conclusions

In this letter we have discussed the π^0 production at MUonE through the process $\mu e \rightarrow \mu e \pi^0$ with the exact tree-level calculation of the matrix element and its implementation in the MC generator MESMER. By studying its numerical impact at the differential level on the distributions relevant for the measurement of the hadronic contribution to the QED running coupling constant, we can conclude that π^0 production is a completely negligible reducible background in view of a target precision of 10ppm. Considering also that pion pair production is kinematically forbidden for realistic event selections, the present study shows that real

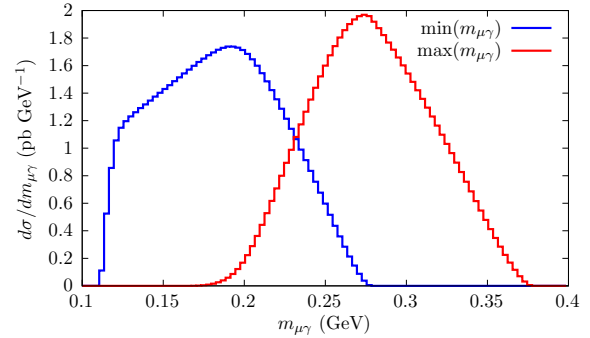


Figure 10: The same as in Fig. 7 but plotted against the minimum (blue curve) and the maximum (red curve) of the invariant mass of the $\mu - \gamma$ system $m_{\mu\gamma}$.

hadron production in μe scattering at the MUonE experiment does not affect the measurement of the QED running coupling constant. The same process $\mu e \rightarrow \mu e \pi^0$ can be of interest for New Physics searches at MUonE involving $2 \rightarrow 3$ channels, in phase space regions complementary to the one of the μe elastic process. For the sake of illustration, we quantified its impact as a background to Z' production in a $L_\mu - L_\tau$ gauge model, as recently suggested in the literature. Through a MC simulation we characterized some relevant distributions involving the photons from π^0 decay, to be considered for a photon veto analysis strategy. Further detailed studies could be performed with the upgraded MC generator MESMER.

5. Acknowledgements

We are sincerely grateful to all our MUonE colleagues for the continuous stimulating collaboration. In particular we thank Mauro Chiesa, Guido

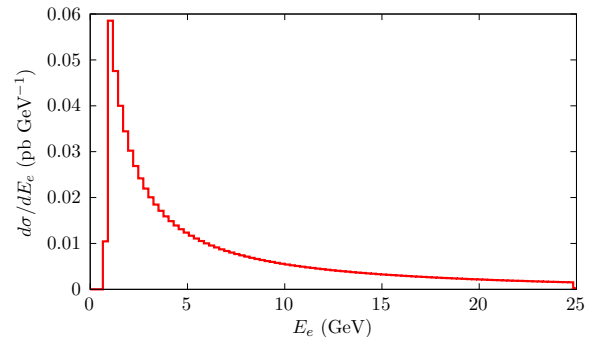


Figure 11: The same as in figure 7 but plotted against the outgoing electron energy E_e .

Montagna and Oreste Nicosini for the valuable discussions and the careful reading of the manuscript.

References

- [1] B. Abi, et al., Measurement of the Positive Muon Anomalous Magnetic Moment to 0.46 ppm, *Phys. Rev. Lett.* 126 (14) (2021) 141801. [arXiv:2104.03281](#), doi: 10.1103/PhysRevLett.126.141801.
- [2] G. W. Bennett, et al., Final Report of the Muon E821 Anomalous Magnetic Moment Measurement at BNL, *Phys. Rev. D* 73 (2006) 072003. [arXiv:hep-ex/0602035](#), doi: 10.1103/PhysRevD.73.072003.
- [3] F. Jegerlehner, A. Nyffeler, The Muon $g-2$, *Phys. Rept.* 477 (2009) 1–110. [arXiv:0902.3360](#), doi: 10.1016/j.physrep.2009.04.003.
- [4] F. Jegerlehner, The Anomalous Magnetic Moment of the Muon, *Springer Tracts Mod. Phys.* 274 (2017) pp. 1–693. doi: 10.1007/978-3-319-63577-4.
- [5] T. Aoyama, et al., The anomalous magnetic moment of the muon in the Standard Model, *Phys. Rept.* 887 (2020) 1–166. [arXiv:2006.04822](#), doi: 10.1016/j.physrep.2020.07.006.
- [6] S. Borsanyi, et al., Leading hadronic contribution to the muon magnetic moment from lattice QCD, *Nature* 593 (7857) (2021) 51–55. [arXiv:2002.12347](#), doi: 10.1038/s41586-021-03418-1.
- [7] C. M. Carloni Calame, M. Passera, L. Trentadue, G. Venanzoni, A new approach to evaluate the leading hadronic corrections to the muon $g-2$, *Phys. Lett. B* 746 (2015) 325–329. [arXiv:1504.02228](#), doi: 10.1016/j.physletb.2015.05.020.
- [8] B. Lautrup, A. Peterman, E. de Rafael, Recent developments in the comparison between theory and experiments in quantum electrodynamics, *Phys. Rept.* 3 (1972) 193–260. doi: 10.1016/0370-1573(72)90011-7.
- [9] E. Balzani, S. Laporta, M. Passera, Hadronic vacuum polarization contributions to the muon $g-2$ in the space-like region (12 2021). [arXiv:2112.05704](#).
- [10] G. Abbiendi, et al., Measuring the leading hadronic contribution to the muon $g-2$ via μe scattering, *Eur. Phys. J. C* 77 (3) (2017) 139. [arXiv:1609.08987](#), doi: 10.1140/epjc/s10052-017-4633-z.
- [11] A. B. Arbuzov, D. Haidt, C. Matteuzzi, M. Paganoni, L. Trentadue, The Running of the electromagnetic coupling α in small angle Bhabha scattering, *Eur. Phys. J. C* 34 (2004) 267–275. [arXiv:hep-ph/0402211](#), doi: 10.1140/epjc/s2004-01649-0.
- [12] G. Abbiendi, et al., Measurement of the running of the QED coupling in small-angle Bhabha scattering at LEP, *Eur. Phys. J. C* 45 (2006) 1–21. [arXiv:hep-ex/0505072](#), doi: 10.1140/epjc/s2005-02389-3.
- [13] A. Anastasi, et al., Measurement of the running of the fine structure constant below 1 GeV with the KLOE Detector, *Phys. Lett. B* 767 (2017) 485–492. [arXiv:1609.06631](#), doi: 10.1016/j.physletb.2016.12.016.
- [14] G. Abbiendi, et al., Letter of Intent: the MUonE project, *Tech. Rep. CERN-SPSC-2019-026*, SPSC-I-252, CERN, Geneva (Jun 2019). URL <https://cds.cern.ch/record/2677471>
- [15] G. Abbiendi, et al., Results on multiple Coulomb scattering from 12 and 20 GeV electrons on carbon targets, *JINST* 15 (01) (2020) 01. [arXiv:1905.11677](#), doi: 10.1088/1748-0221/15/01/P01017.
- [16] G. Ballerini, et al., A feasibility test run for the MUonE project, *Nucl. Instrum. Meth. A* 936 (2019) 636–637. doi: 10.1016/j.nima.2018.10.148.
- [17] G. Abbiendi, et al., A study of muon-electron elastic scattering in a test beam, *JINST* 16 (06) (2021) P06005. [arXiv:2102.11111](#), doi: 10.1088/1748-0221/16/06/P06005.
- [18] G. Abbiendi, Status of the MUonE experiment, *PoS ICHEP2020* (2021) 223. [arXiv:2012.07016](#), doi: 10.22323/1.390.0223.
- [19] G. Abbiendi, et al., Mini-Proceedings of the STRONG2020 Virtual Workshop on “Space-like and Time-like determination of the Hadronic Leading Order contribution to the Muon $g - 2$ ”, 2022. [arXiv:2201.12102](#).
- [20] G. Abbiendi, Status of the MUonE experiment, in: 10th International Conference on New Frontiers in Physics, 2022. [arXiv:2201.13177](#).
- [21] P. Mastrolia, M. Passera, A. Primo, U. Schubert, Master integrals for the NNLO virtual corrections to μe scattering in QED: the planar graphs, *JHEP* 11 (2017) 198. [arXiv:1709.07435](#), doi: 10.1007/JHEP11(2017)198.
- [22] M. Alacevich, C. M. Carloni Calame, M. Chiesa, G. Montagna, O. Nicosini, F. Piccinini, Muon-electron scattering at NLO, *JHEP* 02 (2019) 155. [arXiv:1811.06743](#), doi: 10.1007/JHEP02(2019)155.
- [23] S. Di Vita, S. Laporta, P. Mastrolia, A. Primo, U. Schubert, Master integrals for the NNLO virtual corrections to μe scattering in QED: the non-planar graphs, *JHEP* 09 (2018) 016. [arXiv:1806.08241](#), doi: 10.1007/JHEP09(2018)016.
- [24] T. Engel, A. Signer, Y. Ulrich, A subtraction scheme for massive QED, *JHEP* 01 (2020) 085. [arXiv:1909.10244](#), doi: 10.1007/JHEP01(2020)085.
- [25] P. Banerjee, et al., Theory for muon-electron scattering @ 10 ppm: A report of the MUonE theory initiative, *Eur. Phys. J. C* 80 (6) (2020) 591. [arXiv:2004.13663](#), doi: 10.1140/epjc/s10052-020-8138-9.
- [26] C. M. Carloni Calame, M. Chiesa, S. M. Hasan, G. Montagna, O. Nicosini, F. Piccinini, Towards muon-electron scattering at NNLO, *JHEP* 11 (2020) 028. [arXiv:2007.01586](#), doi: 10.1007/JHEP11(2020)028.
- [27] P. Banerjee, T. Engel, A. Signer, Y. Ulrich, QED at NNLO with McMule, *SciPost Phys.* 9 (2020) 027. [arXiv:2007.01654](#), doi: 10.21468/SciPostPhys.9.2.027.
- [28] E. Budassi, C. M. C. Calame, M. Chiesa, C. L. Del Pio, S. M. Hasan, G. Montagna, O. Nicosini, F. Piccinini, NNLO virtual and real leptonic corrections to muon-electron scattering, *JHEP* 11 (9 2021). [arXiv:2109.14606](#), doi: 10.1007/JHEP11(2021)098.
- [29] R. Bonciani, et al., The two-loop four-fermion scattering amplitude in QED (6 2021). [arXiv:2106.13179](#).
- [30] M. Fael, Hadronic corrections to μe scattering at NNLO with space-like data, *JHEP* 02 (2019) 027. [arXiv:1808.08233](#), doi: 10.1007/JHEP02(2019)027.
- [31] M. Fael, M. Passera, Muon-Electron Scattering at Next-To-Next-To-Leading Order: The Hadronic Corrections, *Phys. Rev. Lett.* 122 (19) (2019) 192001. [arXiv:1901.03106](#), doi: 10.1103/PhysRevLett.122.192001.
- [32] A. Masiero, P. Paradisi, M. Passera, New physics at the MUonE experiment at CERN, *Phys. Rev. D* 102 (7) (2020) 075013. [arXiv:2002.05418](#), doi: 10.1103/PhysRevD.102.075013.

- [33] P. S. B. Dev, W. Rodejohann, X.-J. Xu, Y. Zhang, MUonE sensitivity to new physics explanations of the muon anomalous magnetic moment, JHEP 05 (2020) 053. [arXiv:2002.04822](#), [doi:10.1007/JHEP05\(2020\)053](#).
- [34] K. Asai, K. Hamaguchi, N. Nagata, S.-Y. Tseng, J. Wada, Probing the L_μ - L_τ Gauge Boson at the MUonE Experiment (9 2021). [arXiv:2109.10093](#).
- [35] I. Galon, D. Shih, I. R. Wang, Dark Photons and Displaced Vertices at the MUonE Experiment (2 2022). [arXiv:2202.08843](#).
- [36] S. J. Brodsky, T. Kinoshita, H. Terazawa, Two Photon Mechanism of Particle Production by High-Energy Colliding Beams, Phys. Rev. D 4 (1971) 1532–1557. [doi:10.1103/PhysRevD.4.1532](#).
- [37] C. Patrignani, et al., Review of Particle Physics, Chin. Phys. C 40 (10) (2016) 100001. [doi:10.1088/1674-1137/40/10/100001](#).
- [38] H. Czyż, P. Kiszka, S. Tracz, Modeling interactions of photons with pseudoscalar and vector mesons, Phys. Rev. D 97 (1) (2018) 016006. [arXiv:1711.00820](#), [doi:10.1103/PhysRevD.97.016006](#).
- [39] M. Tanabashi, et al., Review of Particle Physics, Phys. Rev. D 98 (3) (2018) 030001. [doi:10.1103/PhysRevD.98.030001](#).
- [40] J. A. M. Vermaseren, New features of FORM (10 2000). [arXiv:math-ph/0010025](#).
- [41] J. Kuipers, T. Ueda, J. A. M. Vermaseren, J. Vollinga, FORM version 4.0, Comput. Phys. Commun. 184 (2013) 1453–1467. [arXiv:1203.6543](#), [doi:10.1016/j.cpc.2012.12.028](#).
- [42] B. Ruijl, T. Ueda, J. Vermaseren, FORM version 4.2 (2017). [arXiv:1707.06453](#).
- [43] F. A. Berends, R. Pittau, R. Kleiss, All electroweak four fermion processes in electron - positron collisions, Nucl. Phys. B 424 (1994) 308–342. [arXiv:hep-ph/9404313](#), [doi:10.1016/0550-3213\(94\)90297-6](#).
- [44] B. P. Kersevan, E. Richter-Was, Improved phase space treatment of massive multi-particle final states, Eur. Phys. J. C 39 (2005) 439–450. [arXiv:hep-ph/0405248](#), [doi:10.1140/epjc/s2004-02105-y](#).
- [45] H. Czyż, S. Ivashyn, EKHARA: A Monte Carlo generator for e^+e^- to $e^+e^- \pi^0$ and e^+e^- to $e^+e^- \pi^+ \pi^-$ processes, Comput. Phys. Commun. 182 (2011) 1338–1349. [arXiv:1009.1881](#), [doi:10.1016/j.cpc.2011.01.029](#).
- [46] H. Czyż, P. Kiszka, EKHARA 3.0: an update of the EKHARA Monte Carlo event generator, Comput. Phys. Commun. 234 (2019) 245–255. [arXiv:1805.07756](#), [doi:10.1016/j.cpc.2018.07.021](#).